



EFFECTS OF INITIAL STATIC SHEAR ON THE BEHAVIOR OF PARTIALLY AND FULLY SATURATED INAGI SAND

Jeanelle FEVRIER¹, Takeshi SATO², Gabriele CHIARO³ and Junichi KOSEKI⁴

ABSTRACT: Many slope failures are usually caused by rainfall or earthquake motion. It is well known that saturated slopes are in general dangerous and susceptible to failure. On the other hand, the behavior of partially saturated slopes subjected to earthquake loading is not very well understood. This paper presents an experimental study of the effects of initial static shear stress on the undrained cyclic loading behavior of partially and fully saturated Inagi sand specimens. The study was carried out using a double-cell type triaxial test apparatus capable of measuring the volume change, the pore air pressure and pore water pressure of partially saturated specimens. The emphasis of this study was placed on medium dense to dense Inagi sand specimens by carrying out undrained cyclic loading triaxial tests, where different values on initial static shear stress (representative of the sloped ground) were introduced into the specimens by means of anisotropic consolidation before the application of undrained cyclic loading. The study revealed that, under the conditions employed for the tests on partially saturated Inagi sand specimens, a small value of initial static shear applied in compression proved to be advantageous to liquefaction resistance but high levels of initial static shear may prove to be an unfavorable factor. In contrast, in the case of fully saturated Inagi sand specimens the introduction of initial static shear stress proved to be detrimental to liquefaction resistance.

Key Words: initial static shear, matric suction, net stress, pore air pressure compression, liquefaction resistance

INTRODUCTION

For many years, it has been thought that liquefaction only occurred in saturated sands, and though loose, saturated cohesionless soils tend to be more vulnerable to a loss of soil strength under cyclic loading (i.e. earthquake motion), there is supporting evidence which implies that soils containing fines such as silty sands under partially saturated conditions may also be susceptible to liquefaction (Ngo, 2009; among others).

¹ Graduate Student, Department of Civil Engineering, University of Tokyo

² Technical Director, Integrated Geotechnology Institute Ltd.

³ Associate Research Fellow, University of Wollongong, Australia

⁴ Professor, Institute of Industrial Science, University of Tokyo

Due to the various challenges that have arisen as a result of the implementation of traditional soil mechanics in the present day issues faced in the field of geotechnical engineering under this particular soil condition, the study on the behavior of partially saturated soils has now become the subject of numerous ongoing studies in recent decades, and though several researchers have written and contributed to the field of knowledge of unsaturated soils there is still a great need to better understand the behavior of these soils subjected to earthquake loading.

Moreover, it has been observed from past studies and also case histories of past earthquakes that soil elements beneath a sloped surface or leveled ground underneath structures are subjected to initial static stresses on the horizontal plane. During the event of an earthquake, these elements are subjected to an additional cyclic shear stress due to the vertically upward propagation of shear waves from the bedrock as a result of the earthquake motion. The presence of these initial static shear stresses can have a major effect on the response of the soil to a superimposed cyclic loading. Thus it is necessary to observe the effects that initial static shear would have on partially saturated soils.

In view of the above the objective of this study has been set to gain insight into the effects of initial static shear on the undrained cyclic behavior of partially and fully saturated Inagi sand specimens. In this paper, the results obtained from conducting a series of tests including isotropic consolidation tests, anisotropic consolidation tests (in this stage a specified value of initial static shear stress representative of the existing conditions of sloped ground was introduced into the specimen) and undrained cyclic loading tests are presented.

MATERIAL, TEST APPARATUS AND EXPERIMENTAL PROCEDURE

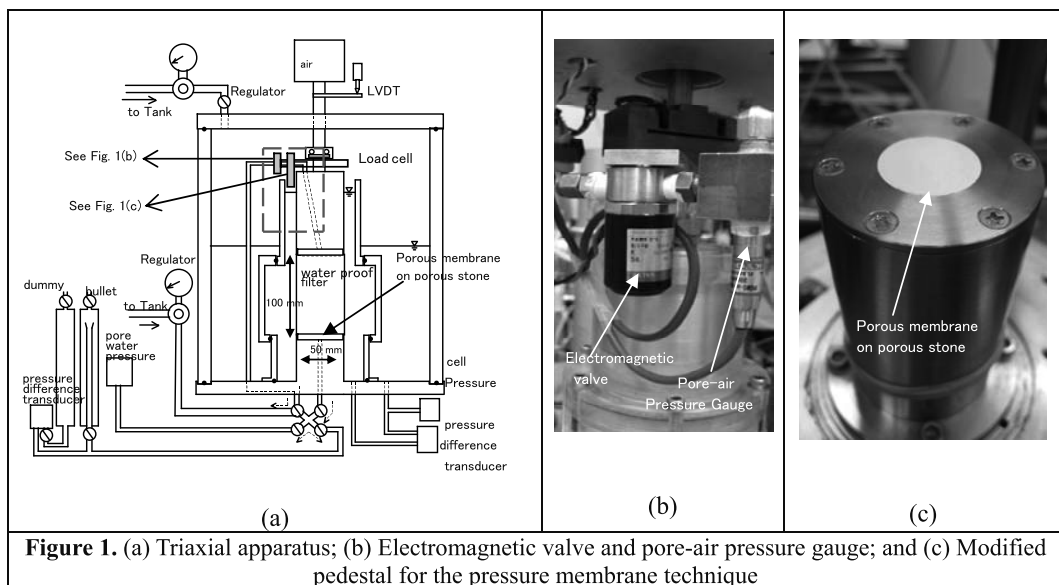
In the case of this study the test material used was Inagi sand. It is inland weathered sand widely found in the Tama district, Tokyo, Japan. This sand consists of crushable particles and can be classified as silty sand with a considerable amount of fines under $75\mu\text{m}$, $F_c = 17.9\%$ with $G_s = 2.600$; $\rho_{d\text{max}} = 1.393 \text{ g/cm}^3$ and $\rho_{d\text{min}} = 1.004 \text{ g/cm}^3$. Several cylindrical specimens having dimensions of 50mm in diameter and about 100mm in height were prepared by the wet tamping method in ten (10) layers. The relative density of the soil specimens after isotropic consolidation ranged from 54 to 70% with the degree of saturation, S_r , ranging from 67 to 100 % as typically shown in Table 1.

Since the main objective of this study is to observe the effects of initial static shear on the undrained cyclic behavior of partially saturated Inagi sand, a double-cell type triaxial test apparatus was employed. A schematic layout of this testing apparatus is shown in Fig. 1(a). This apparatus is capable of measuring the volume change, the pore air pressure and pore water pressure of partially saturated specimens. This double-cell type triaxial apparatus is unique in its kind with respect to other triaxial test apparatuses as a result of three special features: (1) a special electromagnetic valve and a pore air pressure gauge attached to the top cap as shown in Fig. 1(b) which is used to measure the pore-air pressure readings, (2) a pedestal as shown in Fig. 1(c) which allows for the employment of the pressure membrane technique which was found to be effective in controlling and/or measuring the matric suction (Nishimura et al, 2009) and (3) cell pressure control which helps in the case of the partially saturated tests to maintain the total mean principal stress constant during cyclic loading.

The specimens were initially consolidated isotropically and then consolidated anisotropically by applying a prescribed static axial stress until 60kPa mean principal stress in terms of net stress, $p_{\text{net}} = p - u_a$ (where $p = (\sigma_a + 2\sigma_r)/3$ and u_a is the pore-air pressure) and desired values of initial static shear stress (representative of the slope inclination) were achieved. Finally a sinusoidal cyclic axial load was then applied at a frequency of 0.1Hz under undrained conditions.

Table 1. Test conditions for fully and partially saturated Inagi sand specimens.

Test #	Sr (%)	Dr (%)	q_{evc} (kPa)	q_{st} (kPa)	$p_{net,0}$ (kPa)	CSR ($q_{evc} / 2 p_{net,0}$)
FS6c	100	61.8	36	0	60	0.30
FS2c	100	60.1	30	0	60	0.25
FS3c	100	61.9	24	0	60	0.20
FS57c	100	69.2	18	0	60	0.15
FS39c	100	69.9	48	15	60	0.40
FS40c	100	66.0	36	15	60	0.30
FS41c	100	63.3	30	15	60	0.25
FS45c	100	68.0	24	15	60	0.20
FS46c	100	64.9	18	15	60	0.15
FS38c	100	62.3	42	30	60	0.35
FS42c	100	66.0	30	30	60	0.25
FS43c	100	66.5	24	30	60	0.20
FS44c	100	66.5	18	30	60	0.15
FS58c	100	67.8	12	30	60	0.10
PS47c	66.5	53.6	54	0	60	0.45
PS48c	66.7	58.1	48	0	60	0.40
PS49c	69.8	56.7	42	0	60	0.35
PS52c	69.8	58.0	60	15	60	0.50
PS51c	70.0	61.7	54	15	60	0.45
PS56c	70.5	53.5	48	15	60	0.40
PS54c	71.5	60.9	60	30	60	0.50
PS53c	71.3	60.7	54	30	60	0.45
PS55c	70.5	61.4	48	30	60	0.40



TEST RESULTS AND DISCUSSION

Result for medium dense to dense fully and partially saturated Inagi sand specimens without initial static shear stress

Deviator stress

Increasing the angle of slope inclination in compression results in the addition of static compressive deviator stress, q_{static} to the specimen (during anisotropic consolidation) before loading. The undrained cyclic loading then superimposes a periodically changing q_{cyclic} on q_{static} . In the case of Fig. 2(a) shows the typical time histories of axial strain obtained from tests on two specimens FS57c ($D_r = 69.2\%$, fully saturated) and PS47c ($D_r = 53.6\%$, partially saturated) without initial static shear stress ($q_{\text{static}} = 0\text{kPa}$), under otherwise the same test conditions.

Axial Strain

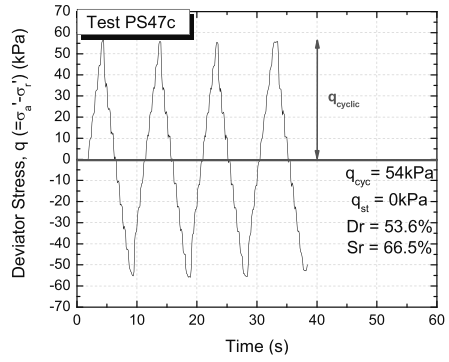
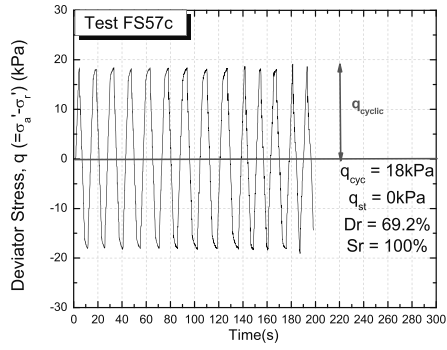
Fig. 2(b) shows the typical time histories of axial strain obtained from tests on two specimens FS57c and PS47c. Specimen PS57c shows an increase in the axial strain as the time increases. Up to the 15th cycle the axial strain accumulates mainly on the triaxial extension side, whilst from the 16th cycle there on, a distribution of axial strain on both the compression side as well as the extension side (though leaning more towards the extension side) is seen. On the other hand in the case of specimen PS47c there is a distribution of axial strain solely on the triaxial extension side.

Stress- strain relationship

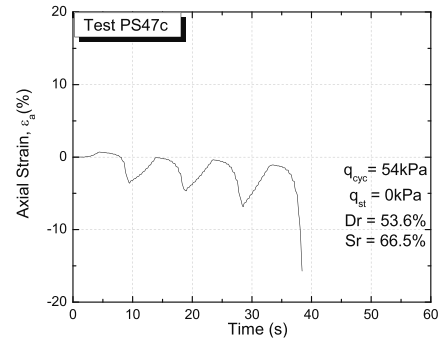
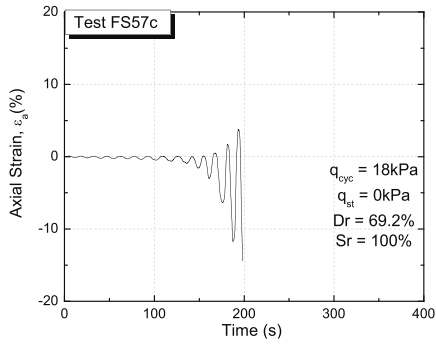
Fig. 2(c) shows the relationship between the deviator stress and the axial strain. In the case of specimen FS57c a gradual accumulation of axial strain on both the triaxial compression side as well as the triaxial extension side can be seen. This coincides with the behavior observed in the axial strain versus time history relationship. Strain softening (i.e., a greater reduction of the effective mean principal stress on the triaxial extension side) similar to that observed in the liquefaction of clean sands can also be seen. However, in the case of specimen PS47c the axial strain is accumulated only on the triaxial extension side.

Effective stress path

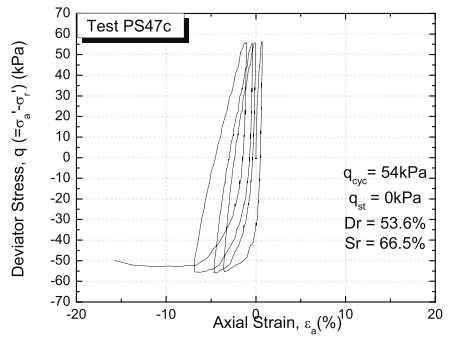
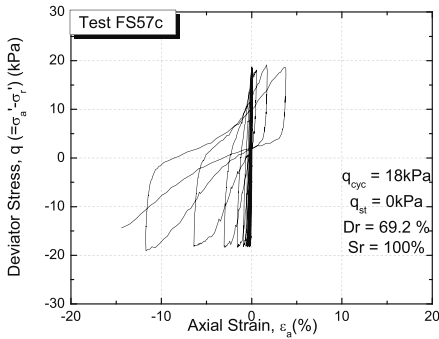
Fig. 2(d) shows the relationship between the deviator stress and the effective mean principal stress. In the case of specimen FS57c though the specimen did not reach an effective mean principal stress value of zero (i.e., $p' = 0\text{kPa}$, full liquefaction), it yielded a failure similar to that seen in liquefaction of clean, loose, saturated sands. A greater reduction of the effective mean principal stress on the triaxial extension side, reaching the failure envelope is also observed. With respect to specimen PS47c though the specimen did not reach full liquefaction with an effective mean principal stress value of zero (i.e., $p' = 0\text{kPa}$), due possibly to anisotropy, a large reduction of effective stress on triaxial extension side accumulated. This seems to be linked with the axial strain behavior that accumulated more predominantly on the extension side.



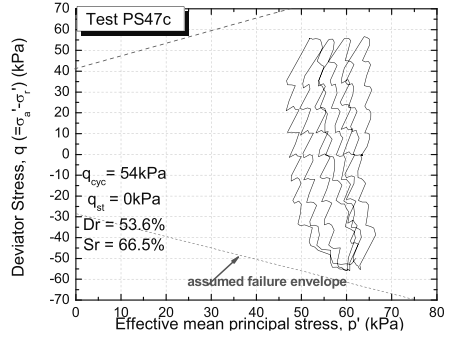
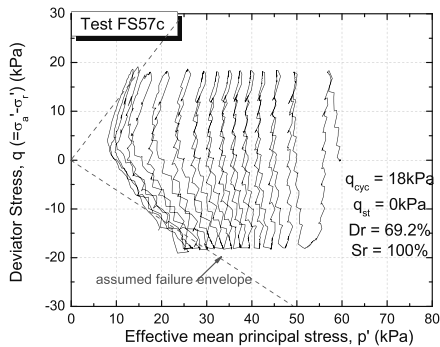
a)



b)



c)



d)

Figure 2. Typical test results on fully and partially saturated specimens without initial static shear in terms of: (a) Deviator stress vs. time, (b) Axial strain vs. time, (c) Stress-strain and (d) Effective stress path relationship

Result for medium dense partially saturated Inagi sand specimens with initial static shear stress

Deviator stress

Increasing the angle of slope inclination in compression results in the addition of static compressive deviator stress, q_{static} to the specimen (during anisotropic consolidation) before loading. The undrained cyclic loading then superimposes a periodically changing q_{cyclic} on q_{static} . In the case of Fig. 3(a) shows the typical time histories of axial strain obtained from tests on two partially saturated specimens PS51c ($Dr = 61.7\%$) and PS53c ($Dr = 60.7\%$) with different initial static shear stresses $q_{\text{static}} = 15\text{kPa}$ and $q_{\text{static}} = 30\text{kPa}$ respectively, under otherwise the same test conditions.

Axial Strain

Fig. 3(b) shows the typical time histories of axial strain obtained from tests on two partially saturated specimens PS51c and PS53c. In the case of specimen PS51c, the shifting of stress states to triaxial compression side was predominant until the 40th cycle, followed by a distribution of axial strain on both the triaxial extension and compression side. On the other hand in the case of specimen PS53c due to the application of relatively large value of initial static shear applied in compression, an accumulation of axial strain towards the compression side with low values of double amplitude axial strain ($\varepsilon_{DA} < 5\%$) was observed.

Pore-air pressure, pore-water pressure, and suction vs. time relationship

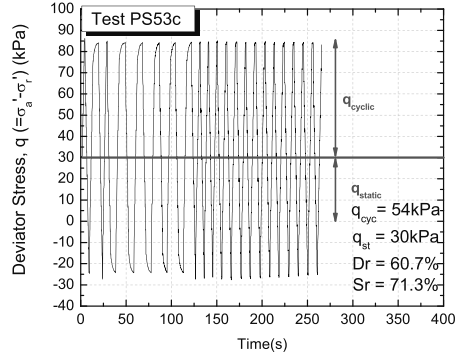
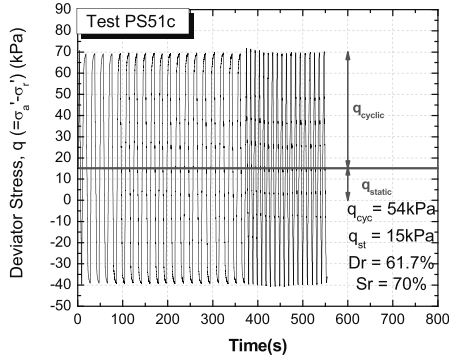
Fig. 3(c) shows the typical time histories for pore-air pressure (u_a), pore-water pressure (u_w) and suction ($u_a - u_w$) obtained from the tests on the two partially saturated specimens PS51c and PS53c respectively. In the case of PS51c an abrupt increase in the pore-air is seen for the first 2 cycles, followed by a gradual increase up to the 50th cycle and then a decrease as the specimens reaches failure. A gradual increase in pore-water pressure is seen throughout. This behavior corresponded to the abrupt increase in the suction for the first 2 cycles followed by a gradually decrease until the 35th cycle and then a gradual increase again. On the other hand in the case of specimen PS53c there are a gradual increase in the pore-water pressure and the pore-air pressure throughout. This behavior corresponded to the almost constant increase observed in the suction behavior.

Stress- strain relationship

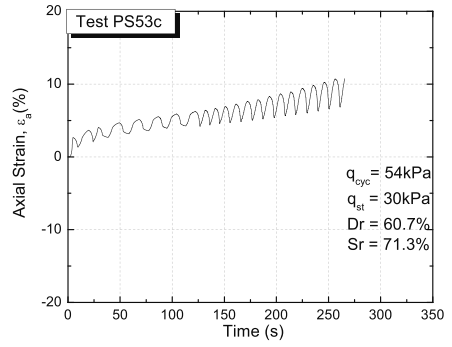
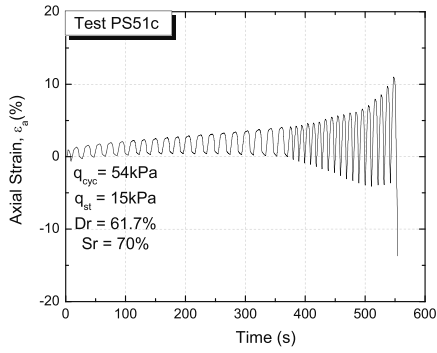
Fig. 3(d) shows the relationship between the deviator stress and the axial strain. In the case of specimen PS51c there is an accumulation of axial strain on both the triaxial extension and compression side. On the other hand in the case of specimen PS53c due to the application of a relatively large value of initial static shear in compression, a predominant accumulation of axial strain on the compression side was observed.

Effective stress path

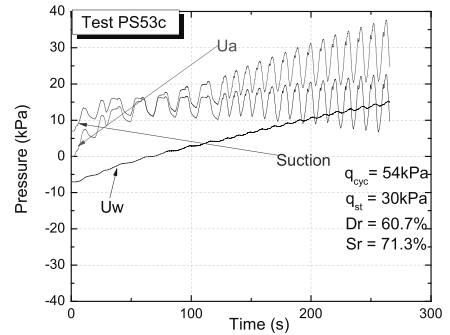
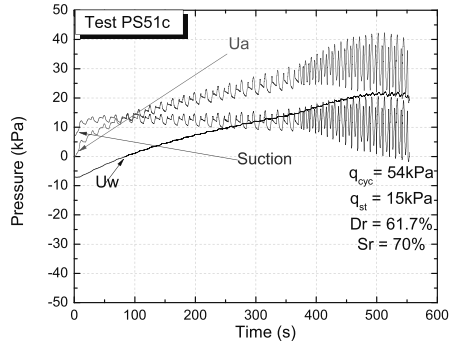
Fig. 3(e) shows the relationship between the deviator stress ($q = \sigma'_a - \sigma'_r$) and the effective mean principal stress ($p' = p_{\text{net}} - u_a + \chi(u_a - u_w)$). In the case of specimen PS51c there is no significant reduction of effective mean principal stress observed on either side (whether extension or compression) as a result of the specimen reaching failure on both the triaxial extension and triaxial compression side and thus the resistance against undrained cyclic loading was very high. On the other hand in the case of specimen PS53c due to the application of a relatively large value of initial static shear in compression, a large reduction of effective mean principal stress on the compression side reaching the failure envelope.



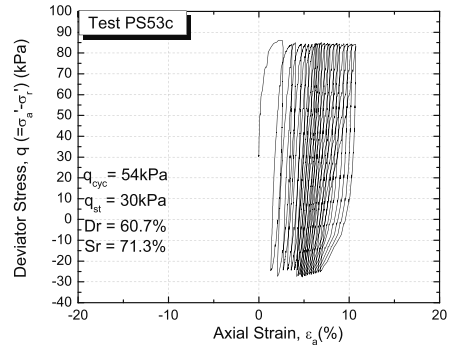
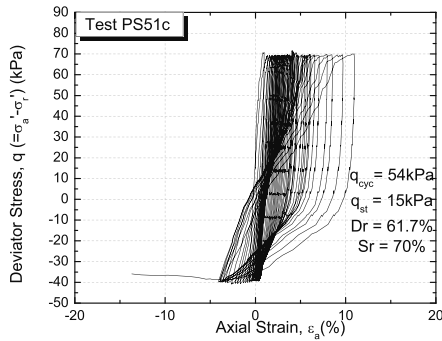
a)



b)



c)



d)

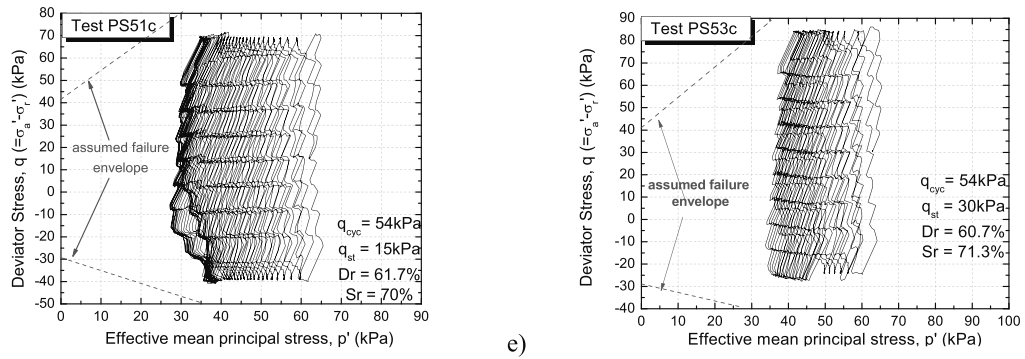


Figure 3. Typical test results on partially saturated specimens with initial static shear in terms of: (a) Deviator stress vs. time, (b) Axial strain vs. time, (c) Pore-air pressure, pore-water pressure, and suction vs. time, (d) Stress-strain and (e) Effective stress path relationship

Discussion of the effects of initial static shear stress on the undrained cyclic loading behavior of partially and fully saturated Inagi sand specimens

The relationship between cyclic stress ratio versus number of cycle

In the case of this study, the resistance against liquefaction (or more strictly, resistance against cyclic strain accumulation) is evaluated in terms of number of cycles required to develop a specific amount of single amplitude axial strain, $\epsilon_{SA} = 5\%$. Fig. 4 and Fig. 5 depicts the relationship between cyclic stress ratio and the number of cycles, N_c , to cause a single amplitude axial strain, which is defined referring to the state immediately before the cyclic loading, ϵ_{SA} of 5%, for cases with $p_{net,0} = 60\text{kPa}$. In Fig. 4 and Fig. 5 it is observed that for each range of initial static shear stress the fully saturated specimens tend to have a lower cyclic stress ratio in comparison to the partially saturated specimens. With respect to the specimens (both fully and partially saturated) without initial static shear it was observed that a decrease in the degree of saturation from 100% to 70%, caused the cyclic stress ratio to be increased by a factor of 2.4. In case of the fully saturated specimens the samples having an initial static shear stress of 30kPa tend to have a lower value of cyclic stress ratio than that of the case with no initial static shear stress. Whilst the specimens with an initial static shear stress of 15kPa in most cases (i.e., from $CSR = 0.4 \sim 0.2$) tend to have a higher liquefaction resistance than that of the cases with no initial static shear stress.

Focusing on the partially saturated specimens it is observed that a small increase in the initial static shear stress (i.e., from 0 to 15kPa) can prove to be beneficial for liquefaction resistance, however a further increase in the initial static shear stress (i.e., from 15 to 30kPa) can cause a decrease in the liquefaction resistance (though the decrease was not lower than the value obtained for that of the case where there was no initial static shear stress).

Lee & Seed (1967) discovered that an increase in the initial static shear stress results in an increase in the liquefaction resistance based on cyclic triaxial compression tests on anisotropically consolidated samples. However, in the case of this study as observed in Fig. 6 with respect to partially saturated soils specimens, though an increase in the liquefaction resistance was observed as the initial static shear stress increased; this behavior however, was not dominant for all values of initial static shear stress. On the other hand in the case of the fully saturated specimens an introduction of initial static shear proved to be detrimental to liquefaction resistance.

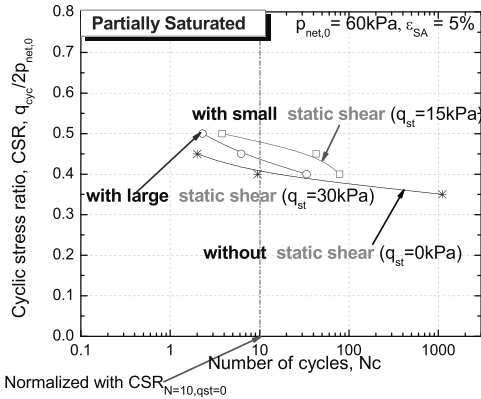


Figure 4. Effect of initial static shear stress on cyclic stress ratio required to cause 5% single amplitude axial strain ($\epsilon_{SA} = 5\%$) in medium dense to dense fully saturated Inagi sand

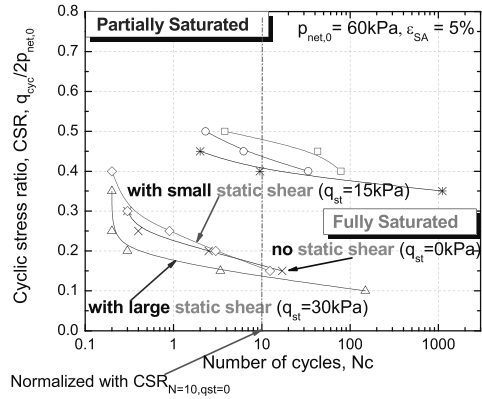


Figure 5. Effect of initial static shear stress on cyclic stress ratio required to cause 5% single amplitude axial strain ($\epsilon_{SA} = 5\%$) in medium dense partially saturated Inagi sand

The relationship between normalized cyclic stress ratio versus initial static shear stress

The effects of the introduction of initial static shear on the undrained cyclic loading behavior of partially and fully saturated Inagi sand specimens was singled out by plotting $SR_{N=10}/SR_{N=10, qst=0}$ against the initial static shear stress, as shown in Fig. 6, (which depicts the effect of initial static shear stresses on cyclic stress ratio required to cause various levels of strain in 10cycles). Focusing on partially saturated specimens it was observed that increasing the initial static stress from 0kPa to 15kPa resulted in an increase in the normalized cyclic stress ratio. However, this favorable effect was not maintained under any value of initial static shear stress. As q_{static} increased to a higher level (from 15kPa to 30kPa), the normalized cyclic stress ratio began to drop. Nevertheless this drop did not go below than that of the case where there is an absence of initial static shear stress (i.e., $q_{static}=0$ kPa). On the other hand, the effects on initial static shear on the undrained cyclic behavior of fully saturated Inagi sand specimens proved to be quite detrimental. The introduction of an initial static shear stress of 15kpa resulted in a decrease in the normalized cyclic stress ratio and further increasing the value of initial static shear from 15kPa to 30kPa caused the normalized cyclic stress ratio to be less than that at $q_{static}=0$ kPa.

The results obtained in Fig. 6 also revealed that the common belief that the presence of initial static shear stress always increases (according to Lee & Seed, 1967) the resistance to liquefaction or cyclic strain development when compared to the case of no static shear was not always found to be legitimate. These results corresponded to the observations made by Vaid and Chern (1983), Hyodo et al. (1991), Yang and Sze (2011) among others who concluded from their investigations that resistance against liquefaction and/or cyclic strain accumulation could either increase or decrease depending on the combined effects of static and cyclic shear stresses, the type of loading applied (i.e., reversal, non-reversal or intermediate), the type of failure (cyclic or rapid liquefaction, and residual deformation) and the relative density as well as the confining stress.

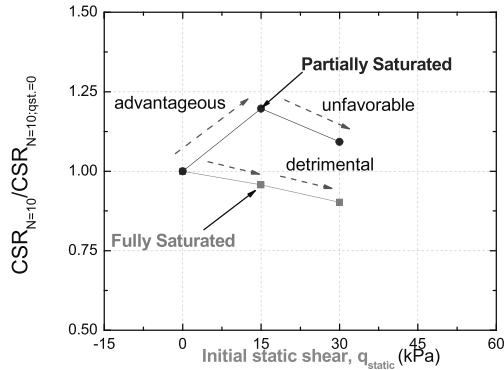


Figure 6. Effect of initial static shear stress on cyclic stress ratio required to cause various levels of strain ($\epsilon_{SA}=5\%$) in 10cycles

SUMMARY AND CONCLUSIONS

In this paper, the experimental investigation into the effects of initial static shear stress on the undrained cyclic loading behavior of partially and fully saturated specimens are presented. In this study partially saturated as well as fully saturated Inagi sand specimens were subjected to undrained cyclic loading combined with different values of initial static shear stress in order to observe and to gain a more in-depth understanding of the behavior of partially saturated soil slopes during earthquakes. The results from these series of tests can be summarized as follows: (1) a decrease in the degree of saturation from 100% to 70%, caused the cyclic stress ratio to be increased by a factor of 2.4. This increase in cyclic resistance of *partially saturated* soils is as a result of the effects caused by *matric suction* and *pore air compression*; (2) in the case of *partially saturated* soils a small *static shear stress* (in the case of this study $q_{static}=15\text{kPa}$) applied in compression was *advantageous* to liquefaction resistance but high levels of initial static shear stress (in the case of this study $q_{static}=30\text{kPa}$) may become an *unfavorable* factor; (3) with respect to *fully saturated* soils the introduction of *initial static shear stress* ($q_{static}=15\text{kPa}$, 30kPa) proved to be *detrimental* to liquefaction resistance.

It is therefore concluded that the presence of initial static shear stress does not always increase the resistance to liquefaction or cyclic strain development. The resistance against liquefaction and/or cyclic strain accumulation could either increase or decrease depending on the combined effects of static and cyclic shear stresses, the type of loading applied (i.e., reversal, non-reversal or intermediate), the type of failure (cyclic or rapid liquefaction, and residual deformation) and the relative density as well as the confining stress.

REFERENCES

- Chiaro, G., (2010). "Deformation properties of sand with initial static shear in undrained cyclic torsional shear tests and their modeling" Doctoral thesis, Dep. of Civil Engineering, The University of Tokyo
- Hyodo, M., Murata, H., Yasufuku, N. and Fujii, T. (1991): "Undrained cyclic shear strength and residual shear strain of saturated sand by cyclic triaxial tests", *Soils and Foundations*, 31 (3), 60-76
- Lee, K. D. and Seed, H. B. (1967a): "Cyclic stress conditions causing liquefaction of sand", *Journal of Soil Mechanics and Foundation Division, ASCE*, 93 (SM5), 47-70
- Lee, K. D. and Seed, H. B. (1967b): "Dynamic strength of anisotropically consolidated sand", *Journal*

of Soil Mechanics and Foundation Division, ASCE, 93 (SM5), 169-190

Ngo Tuan Anh, (2009). "Undrained cyclic triaxial tests on partially saturated Inagi sand under controlled cell pressure." *Master thesis, Dep. of Civil Engineering, The University of Tokyo*, (in Japanese)

Nishimura, T., Toyota, H. and Koseki, J., (2009). "Evaluation of apparent cohesion of an unsaturated soil", *Proceedings of the 4th Asia Pacific Conference on Unsaturated Soils*. New Castle, Australia.

Vaid, Y. P. and Chern, J.C. (1983): "Effects of static shear on resistance to liquefaction", *Soils and Foundations, 23 (1)*, 47-60

Yang, J. and Sze, H. Y. (2011): "Cyclic behavior and resistance of saturated sand under non-symmetrical loading conditions." *Geotechnique 61*, No.1, 59-73

